Mechanistic Study of Oxygen-Transfer Reaction Catalyzed by an Oxorhenium(V) Compound

Ruili Huang and James H. Espenson*

Ames Laboratory and the Department of Chemistry, Iowa State University of Science and Technology, Ames, Iowa 50011

Received July 31, 2000

The new binuclear oxothiolatorhenium(V) compound, $Re_2O_2(mtp)_3$ (**D_1**, $mtpH_2$ = 2-mercaptomethylthiophenol) was found to be an efficient catalyst for oxygen-transfer reactions. Strong Lewis bases such as phosphines coordinate to one of the rhenium centers in **D_1**; we suggest that this opens one of the Re−S bridges. Dialkylsulfides coordinate weakly to **D_1**. Alkylarylsulfides, diarylsulfides, triphenylarsine and triphenylstibine, and dienes and alkenes do not coordinate to **D_1**. **D_1** catalyzes the oxidation of phosphines, arsines, stibenes, sulfides, and dienes by pyridine *N*-oxides and catalyzes the oxidation of phosphines by dimethyl sulfoxide. The kinetics and mechanism for the oxidation of triarylphosphines by pyridine *N*-oxides were investigated. The relative reactivities of all substrates were studied by competitive reactions. The order was found to be phosphine > arsine > stibene > sulfide > diene. The reaction is proposed to go through a Re(VII) intermediate with pyridine *N*-oxide as one of the ligands. The N−O bond was activated through coordination to rhenium, and the oxygen atom was abstracted by a phosphine forming a phosphine oxide.

Introduction

Oxygen-atom-transfer reactions are catalyzed by high-valent transition metal−oxo complexes, such as Re^{VII}/Re^{V},[1−12] Mo^{VI}/Mo^{IV},[13,14] Mo^{VI}/Mo^{IV},[13,14] and W^{VI}/W^{IV}.[15−19] Molybdenum and tungsten systems have received the most attention because of their roles in biological systems. In such pairs, the oxidation states differ by two units, in keeping with their role as oxotransferases; the metals exist in their highest oxidation states to stabilize the metal−oxo π interaction. The most widely studied rhenium compound is $MeReO_3$ (known as MTO), but in that case (only) a peroxo complex intervenes. A new oxorhenium(V) compound, $(ReO)_2(mtp)_3$ ($mtpH_2$ = 2-mercaptomethylthiophenol) lacking the methyl group found in compounds prepared from MTO, was prepared from Re_2O_7 and $mtpH_2$, which is 2-(mercaptomethyl)thiophenol, according to this equation:[20]

$$Re_2O_7 + 5H_2mtp \rightarrow (ReO)_2(mtp)_3 + 2RS{-}SR + 5H_2O \quad (1)$$

where RS−SR represents the cyclic disulfide from the oxidation of $mtpH_2$. The structure of the dirhenium compound, which we designate **D_1**, has been determined by X-ray crystallography.[20] Its structural formula, presented in Chart 1, bears certain similarities to the formulas of recently reported organometallic

Chart 1. Structural Formulas of Key Compounds

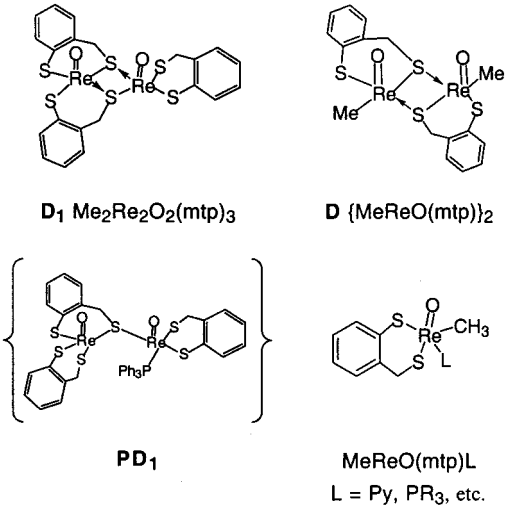

* To whom correspondence should be addressed. E-mail: espenson@iastate.edu.

(1) Owens, G. S.; Arias, J.; Abu-Omar, M. M. *Catal. Today* **2000**, *55*, 317−363.
(2) Yudin, A. K.; Sharpless, K. B. *J. Am. Chem. Soc.* **1997**, *119*, 11536.
(3) Weiner, D. P.; Wiemann, T.; Wolfe, M. M.; Wentworth, P., Jr.; Janda, K. D. *J. Am. Chem. Soc.* **1997**, *119*.
(4) Herrmann, W. A.; Roesky, P. W.; Wang, M.; Scherer, W. *Organometallics* **1994**, *13*, 4531−4535.
(5) Gable, K. P.; Brown, E. C. *Organometallics* **2000**, *19*, 944.
(6) Rybak, W. K.; Zagicek, A. *J. Coord. Chem.* **1992**, *26*, 79.
(7) Dirghangi, B. K.; Menon, M.; Banerjee, S.; Chakravotry, A. *Inorg. Chem.* **1997**, *36*, 1095.
(8) Arterburn, J. B.; Nelson, S. L. *J. Org. Chem.* **1996**, *61*, 2260.
(9) Over, D. E.; Critchlow, S. C.; Mayer, J. M. *Inorg. Chem.* **1992**, *31*, 4643.
(10) Kim, Y.; Gallucci, J.; Wojcicki, A. *J. Am. Chem. Soc.* **1991**, *112*, 8600.
(11) Bryan, J. C.; Stenkamp, R. E.; Tulip, T. H.; Mayer, J. M. *Inorg. Chem.* **1987**, *26*, 2283.
(12) Conry, R. R.; Mayer, J. M. *Inorg. Chem.* **1990**, *29*, 4862−4867.
(13) Hille, R. *Chem. Rev.* **1996**, *96*, 2757−2816.
(14) Johnson, M. K.; Rees, D. C.; Adams, M. M. W. *Chem. Rev.* **1996**, *96*, 2817.
(15) Adams, M. W. W. *Soc. Appl. Microbiol. Symp. Ser.* **1999**, *28*, 108S−117S.
(16) Juszczak, A.; Aono, S.; Adams, M. W. W. *J. Biol. Chem.* **1991**, *266*, 13834−13841.
(17) Schmitz, R. A.; Albracht, S. P. J.; Thauer, R. K. *Eur. J. Biochem.* **1992**, *209*, 1013−1018.
(18) Taya, M.; Hinoki, H.; Kobayashi, T. *Agric. Biol. Chem.* **1985**, *49*, 2513−2515.
(19) Winter, J.; Lerp, C.; Zabel, H. P.; Wildenauer, F. X.; Koenig, H.; Schindler, F. *Syst. Appl. Microbiol.* **1984**, *5*, 457−466.
(20) Huang, R.; Espenson, J. H. Manuscript submitted for publication.

10.1021/ic000854k CCC: $20.00
Published on Web 02/02/2001

compounds with the mtp ligand, such as $\{MeReO(mtp)\}_2$ and $MeReO(mtp)PPh_3$,[21,22] also shown in Chart 1. Such comparisons led us to believe that $\mathbf{D_1}$ might be a useful catalyst for oxygen-atom-transfer reactions. This notion has been verified in several test cases, for the $\mathbf{D_1}$-catalyzed oxidation of phosphines, arsines, stilbenes, dialkyl sulfides, and 1,3-dienes. The last two substrates are notable in that $\{MeReO(mtp)\}_2$ and $MeReO(mtp)PPh_3$ do not catalyze those oxidations. We have undertaken a study of oxygen-atom-transfer reactions catalyzed by $\mathbf{D_1}$, with the greatest emphasis on O-atom transfer from pyridine *N*-oxides (XC_5H_4NO; X = MeO, Me, CN) to phosphines:

$$PyNO + PAr_3 \xrightarrow{\text{catalyst } \mathbf{D_1}} Py + Ar_3PO \qquad (2)$$

Experimental Section

The catalyst $\mathbf{D_1}$ was prepared according to eq 1.[20] The other compounds were obtained commercially. The intensity of the UV−visible absorption spectrum of $\mathbf{D_1}$ is so high that it masks the absorbance changes accompanying the conversion of the substrates to products in eq 2, disallowing spectrophotometric monitoring of the reaction progress. Reactions were followed by ^1H or ^{31}P NMR spectroscopy using a Bruker DRX-400 spectrometer. Benzene-d_6 was the solvent for kinetics measurements, which were carried out mostly at 25.0 °C; a few reactions were studied in toluene-d_8 at −35 °C. Chemical shifts for ^{31}P NMR were referenced to external 85% H_3PO_4. The ^1H NMR chemical shifts were measured relative to the residual proton content of C_6D_5H at δ 7.15 or $C_6D_5CD_2H$ at δ 2.09. The intensities of the proton resonances were measured relative to a known concentration of *tert*-butyl alcohol, used as an internal standard, allowing the conversion of intensities into concentrations. These determinations were carried out under Ar because $\mathbf{D_1}$ reacts with oxygen and also catalyzes the oxidation of phosphines by O_2.[20]

Kinetic Data. Typical of catalytic reactions, Michaelis−Menten kinetics was found rather than a simple mathematical form. Consequently, the method of initial rates was used.[23] The integrated NMR intensities were converted to concentrations; the concentration−time data were then fitted to a typically fifth-order polynomial function by means of the program KaleidaGraph. The initial rate v_i, in units mol L^{-1} s^{-1}, is given by the coefficient m_1:

$$C_t = C_0 - m_1t - m_2t^2 - m_3t^3 ... \qquad (3)$$

Results

Rhenium−Ligand Intermediates. (a) Phosphines and Disulfides. Mixing $\mathbf{D_1}$ and an equimolar amount of any of the phosphines led rapidly to the quantitative formation of an adduct we designate as $\mathbf{PD_1}$ (UV spectra, Figure S-1 of Supporting Information). We were unable to crystallize it and have used ^1H and ^{31}P NMR spectroscopy to show that it contains $\mathbf{D_1}$ and PPh_3 in a 1:1 ratio. For reasons given in the Discussion, we suggest that $\mathbf{PD_1}$ has the structural formula shown in Chart 1. A second phosphine ligand does not coordinate.

On the other hand, $AsPh_3$ and $SbPh_3$ do not coordinate to $\mathbf{D_1}$, possibly for steric reasons. Dimethyl sulfide coordinates to $\mathbf{D_1}$ weakly according to the ^1H NMR spectra, which are broadened upon adding Me_2S. No reaction was observed between $\mathbf{D_1}$ and MeSPh or Ph_2S, which are weaker Lewis bases and, more importantly we believe, larger.

Although the reaction between $\mathbf{D_1}$ and PPh_3 or other phosphines is rapid transformation, it is not instantaneous. A stopped-flow experiment with 25 μmol L^{-1} $\mathbf{D_1}$ and 250 μmol L^{-1} PPh_3 (Figure S-2 of Supporting Information) gave a $t_{1/2}$ of 120 ms. This result shows that $\mathbf{PD_1}$ formation is complete on a time short compared to oxidation; further investigations were not made because it lay outside our objectives for oxidation catalysis. The equilibrium position in this reaction lies far to the right:

$$Re_2O_2(mtp)_3\ (\mathbf{D_1}) + PAr_3 \rightarrow Re_2O_2(mtp)_3{\cdot}PAr_3\ (\mathbf{PD_1}) \qquad (4)$$

NMR spectroscopy was used to characterize the phosphine adducts. Data for eight phosphines were obtained, including $P(p\text{-}YC_6H_4)_3$, PPh_2Me, and $PPhMe_2$. Table 1 summarizes the spectroscopic data used to confirm the formation of the 1:1 adduct (2Re/1P). In these reactions one of the sulfido−rhenium bridges is broken and the dimeric structure is sustained by the one remaining.

Table 1. NMR Chemical Shifts for the Adducts $Re_2O_2(mtp)_3{\cdot}PAr_3$ ($\mathbf{PD_1}$)

	^{31}P NMR (δ/ppm)	
phosphine	$\mathbf{PD_1}$	free phosphine
$P(4\text{-}MeOC_6H_4)_3$	−6.99	−9.31
$P(4\text{-}MeC_6H_4)_3$	−5.98	−6.98
$P(C_6H_5)_3$[a]	−6.64	−4.50
$P(4\text{-}ClC_6H_4)_3$	−7.95	−8.70
$P(4\text{-}CF_3C_6H_4)_3$	−9.10	−5.63
PPh_2Me	−19.21	−26.29
$PPhMe_2$	−34.92	−45.54

[a] Selected ^1H and ^{13}C NMR chemical shifts for $Ph_3P\mathbf{D_1}$ are as follows, with the values in bold showing the group coordinated to Re. ^1H NMR: δ 7.82 (m, 6H, arom, ligand), 7.57 (m, 9H, arom, ligand), 7.70 (d, 1H, arom, J = 8.8 Hz), 7.03−7.55 (m, 10H, arom), 6.78 (d, 1H, arom, J = 7.6 Hz), 4.96 (d, 1H, CH_2, J = 11.6 Hz), **4.94 (d, 1H, CH_2, J = 12.8 Hz)**, **4.62 (d, 1H, CH_2, J = 12.4 Hz)**, 4.54 (d, 1H, CH_2, J = 12.0 Hz), 3.50 (d, 1H, CH_2, J = 11.6 Hz), 3.01 (d, 1H, CH_2), J = 11.6 Hz) ppm. ^{13}C NMR: δ 141.76 (arom), 141.43 (arom), 141.31 (arom), 137.80 (d, arom, ligand, $^1J_{P-C}$ = 312), 137.37 (d, arom, ligand, $^2J_{P-C}$ = 42 Hz), 134.73 (d, arom, ligand, $^3J_{P-C}$ = 35.6 Hz), 132.65 (arom), 132.52 (arom), 132.48 (arom), 132.40 (arom), 131.84 (d, arom, ligand, $^4J_{P-C}$ = 10 Hz), 130.92 (arom), 130.67 (arom), 130.50 (arom), 130.43 (arom), 130.34 (arom), 129.66 (arom), 129.26 (arom), 129.12 (arom), 127.48 (arom), 127.24 (arom), 126.91 (arom), **51.07 (CH_2)**, 41.71 (CH_2), 41.16 (CH_2) ppm.

Rhenium−Ligand Intermediates. (b) Pyridines, Halides, Amines. The addition of a pyridine to $\mathbf{D_1}$ in solution does not lead to $Py\mathbf{D_1}$, however. Instead, irreversible monomerization occurs, forming a new anion, $[ReO(mtp)_2]^-$. Other aspects are less clear: the countercation is an unidentified species containing Re, O, and mtp. The reaction in C_6D_6 and CD_3CN was complete by the time the first ^1H NMR spectrum could be recorded, ca. 1 min. A reaction was carried out using 3.5 mM $P\mathbf{D_1}$ and 15 mM $4\text{-}MeC_5H_4N$ in C_6D_6 at 25 °C, during which $P\mathbf{D_1}$ decomposed entirely in 12 h, yielding 5.2 mM $[ReO(mtp)_2]^-$, 3.5 mM free PPh_3, and 3.6 mM of Py coordinated to an oxorhenium complex. The latter species lacks any NMR signature other than that of Py. Mass balance provides the formula Py_2ReO_x. The initial step appears to be Py coordination to $P\mathbf{D_1}$, which was explored by NMR at 240 K. With equimolar concentrations of Py and $\mathbf{PD_1}$, ^1H and ^{31}P signals of $\mathbf{PD_1}Py_2$ were detected.[24] With more py, the $P\mathbf{D_1}Py_2$ signals first increased and then decreased as signals for free PPh_3, $[ReO(mtp)_2]^-$, and Py_2ReO_x were building up. Excess PyO was then added, which caused $P\mathbf{D_1}Py_2$ to disappear immediately and some Ph_3PO to be formed. As the solution warmed to room temperature, quantitative formation of Ph_3PO was realized.

(21) Jacob, J.; Guzei, I. A.; Espenson, J. H. *Inorg. Chem.* **1999**, *38*, 1040−1041.
(22) Jacob, J.; Lente, G.; Guzei, I. A.; Espenson, J. H. *Inorg. Chem.* **1999**, *38*, 3762−3763.
(23) Hall, K. J.; Quickenden, T. I.; Watts, D. W. *J. Chem. Educ.* **1976**, *53*, 493.

The anion can also be formed from the known[25] compound $[ReO(SPh)_4]^-$ by exchanging the PhS^- ligands with $mtpH_2$, an exchange driven by the relative Lewis basicities of the RS^- ligands and particularly by the chelate effect. This anion was characterized on the basis of mass spectrometry and ^1H and ^{13}C NMR spectroscopies.[26] The same fragmentation of $\mathbf{D_1}$ also occurs with other small ligands, such as amines and halides, added as $[Bu_4N]^+X^-$.

Rhenium−Ligand Intermediates. (c) Pyridine *N*-Oxides and Dimethyl Sulfoxide. The oxidation of $\mathbf{D_1}$ by these oxygen-donor reagents causes the dithiolate ligands to be lost; mostly they are oxidized to the cyclic disulfide of mtp. The rhenium is oxidized to rhenium oxides; the latter material was not simply Re_2O_7 but appeared to contain some residual coordinated mtp as well. Dimethyl sulfide or pyridine are also formed. In C_6D_6, pyridine *N*-oxides react much more rapidly than DMSO, as monitored by ^1H NMR spectroscopy.

Even though pyridine coordinates to $\mathbf{D_1}$ very rapidly, the coordination of pyridine *N*-oxide is ultimately favored. In an experiment with *p*-MeC_5H_4N and *p*-MeC_5H_4NO at the same concentration, $\mathbf{D_1}$ was oxidized to mtp and rhenium oxides by the pyridine *N*-oxide rather than being monomerized by the pyridine. When one adds Py first and PyO immediately thereafter, some $ReO(mtp)_2^-$ was formed, but most of the $\mathbf{D_1}$ was still oxidized.

The reaction between $\mathbf{D_1}$ and PyO was also carried out in the presence of an oxygen-accepting reagent. These included phosphines, sulfides, and 1,3-dienes. In such cases, the O atom transferred to rhenium from PyO or DMSO (O-transfer to phosphine only) was then transferred to the given reagent, which restored $\mathbf{D_1}$. In these cases, therefore, $\mathbf{D_1}$ acts as a catalyst for oxygen transfer. Discovering the reaction scheme for this catalytic cycle and the mechanism by which it takes place are the principal objectives of this research. For that reason, it was important to characterize the interaction between $\mathbf{D_1}$ and PyO. It occurs too rapidly for study by room temperature ^1H NMR spectroscopy, so low-temperature experiments were carried out, as described in the next section. One consequence of this is that $\mathbf{D_1}$ itself is not present at a detectable level during the catalytic oxidation reactions; the "resting state" of the catalyst in phosphine-containing solution is the more stable form, $\mathbf{PD_1}$.

Interaction of $\mathbf{D_1}$ and PyO Studied by Low-Temperature NMR. A solution of $\mathbf{D_1}$ was prepared in toluene-d_8 with excess acetic acid to protonate any pyridine generated from the reaction and to prevent it from coordinating to rhenium. The temperature was adjusted to −35 °C, and PyO was added in small portions with PyO/$\mathbf{D_1}$ ratios of $R = 0.2$, 0.6, 1.5, 2.0, and 4.5. Each solution was monitored at that temperature by ^1H, COSY, and $^1H-^{13}C$ 2-D NMR spectroscopies. With $R < 1$, two $\mathbf{D_1}$−PyO adducts **a** and **b** were formed. The relative intensities of the signals in the NMR spectra[27] were used to show that each species contains a 1:1 ratio of $\mathbf{D_1}$ to PyO. The relative proportions of **a** and **b** were 1.2:1. Free PyO or Py was not detected, and the balance of $\mathbf{D_1}$ remained as such. With PyO, two new species were observed. One is a metastable species designated **I**, which has two PyO coordinated to a single $\mathbf{D_1}$. The other species, formed from **I** and designated **c**, has a single PyO coordinated to a partially oxidized $\mathbf{D_1}$. The aromatic proton signals of the three PyO ligands were clearly resolved for **a**, **b** and **c**, whereas **I** existed only admixed with the other species, thus obscuring the methylene ^1H signals; spectroscopic data for **I** were obtained.[28] As more PyO was added, the signals from **I** decreased and free Py and more of species **c** grew in. Further addition of PyO did not, however, convert **c** into other products. When the temperature was allowed to increase to 25 °C, all of the $\mathbf{D_1}$ derivatives were oxidized to oxorhenium species and the mtp ligands were oxidized to disulfide within 10 min. The reactions involved are summarized in Scheme 1, which presents structures that fit the data and are chemically reasonable but do contain conjectural features. The structural formulas suggested for **a** and **b** may be reversed; they were assigned simply on an assumption of relative Lewis basicities.

O-Atom Transfer: Competitive Oxidation Experiments. Before the results of a direct study of the reaction kinetics are presented, it is useful to consider experiments designed to measure the relative rates of formation of two phosphine oxides when a pair of phosphines was used in a single reaction. In these experiments the concentrations were 0.05−0.10 mM $\mathbf{D_1}$, 30−60 mM PyO, and 2−30 mM of each phosphine, which we represent as P^a and P^b. By NMR, just one $\mathbf{PD_1}$ derivative is present, however, from the strong Lewis base. The concentration of each phosphine oxide, P^aO and P^bO, was determined by integrating the ^1H or ^{31}P NMR signals at various times during the reaction. To analyze these data, let us assume on the basis of the results of kinetics data presented in a subsequent section that the step in which P═O is formed proceeds at a rate given by

$$\frac{d[P^i{=}O]}{dt} = {}^ik[P^i][Int] \qquad (5)$$

in which "Int" represents an intermediate common to each. Two such equations, for P^a and P^b, were divided, giving

$$\frac{d[P^aO]/dt}{d[P^bO]/dt} = \left(\frac{{}^ak}{{}^bk}\right)\frac{[P^a]}{[P^b]} \qquad (6)$$

Integration of eq 6 between the limits $t = 0$ and t gives this expression:

$$\log([P^a]_0 - [P^aO]_t) = \frac{{}^ak}{{}^bk}\log([P^b]_0 - [P^bO]_t) \qquad (7)$$

This method allows the evaluation of the reactivity ratio for any pair of phosphines. The concentration of each phosphine

(24) $\mathbf{PD_1}Py_2$. ^1H NMR: δ 9.07 (d, 2H, Py1, arom), 8.95 (d, 2H, Py2, arom), 6.40 (d, 2H, Py1, arom), 6.29 (d, 2H, Py2, arom), 6.50−7.80 (m, 27H, arom), 5.22 (d, 1H), 5.10 (d, 1H), 4.74 (d, 1H), 4.66 (d, 1H), 4.45 (d, 1H), 3.06 (d, 1H), 1.69 (s, 3H, Py1), 1.63 (s, 3H, Py2). ^{31}P NMR: −5.84 ppm.

(25) Dilworth, J. R.; Neaves, B. D.; Hutchinson, J. P.; Zubieta, J. A. *Inorg. Chim. Acta* **1982**, *65*, L223−L224.

(26) Spectroscopic data in CD_3CN for $[ReO(mtp)_2]^-$ are as follows. ^1H NMR: δ 7.35 (d, 2H, arom, $J = 7.6$), 7.27 (d, 2H, arom, $J = 7.6$ Hz), 7.16 (t, 2H, arom, $J = 7.2$ Hz), 7.08 (t, 2H, arom, $J = 7.2$ Hz), 4.74 (d, 2H, CH_2, $J = 11.6$ Hz), 3.25 (d, 2H, CH_2 $J = 12.0$ Hz) ppm. ^{13}C NMR: δ 133.18 (arom), 133.08 (arom), 130.65 (arom), 130.53 (arom), 40.00 (CH_2) ppm. MS (ESI): *m*/*z* 510 (anion).

(27) ^1H NMR spectra in toluene-d_8 at −35 °C for *p*-MePyO$\mathbf{D_1}$ adducts **a**, **b**, and **c**. d/ppm, **a**: δ 9.06 (d, 2H, arom), 8.0−6.5 (m, 12H, arom), 6.42 (d, 2H, arom), 5.06 (d, 1H), 4.65 (d, 1H), 4.42 (d, 1H), 4.27 (d, 1H), 3.29 (d, 1H), 3.01 (d, 1H), 1.77 (s, 3H) ppm. **b**: δ 8.93 (d, 2H, arom), 8.0−6.5 (m, 12H, arom), 6.30 (d, 2H, arom), 5.18 (d, 1H), 4.74 (d, 1H), 4.72 (d, 1H), 4.51 (d, 1H), 4.34 (d, 1H), 4.18 (d, 1H), 1.75 (s, 3H) ppm. **c**: δ 8.80 (d, 2H, arom), 8.0−6.5 (m, 12H, arom), 6.62 (d, 2H, arom), 5.10 (d, 1H), 4.80 (d, 1H), 4.61 (d, 1H), 4.38 (d, 1H), 3.94 (d, 1H), 3.69 (d, 1H), 1.92 (s, 3H) ppm.

(28) ^1H NMR spectra in toluene-d_8 at −35 °C for *p*-MePyO$\mathbf{D_1}$ adduct **I** (aromatic protons of coordinated *p*-MePyO), free *p*-MePyO, and *p*-$MePyH^+$. **I**: δ 8.63 (d, 2H, arom), 6.25 (d, 2H, arom), 8.85 (d, 2H, arom), 6.38 (d, 2H, arom) ppm. *p*-MePyO: δ 8.36 (d, 2H, arom), 6.39 (d, 2H, arom), 32.35 (s, 33H) ppm. *p*-$MePyH^+$: δ 38.26 (d, 32H, arom), 36.06 (d, 32H, arom), 31.44 (s, 33H) ppm.

Scheme 1. Reactions between $\mathbf{D_1}$ and PyO

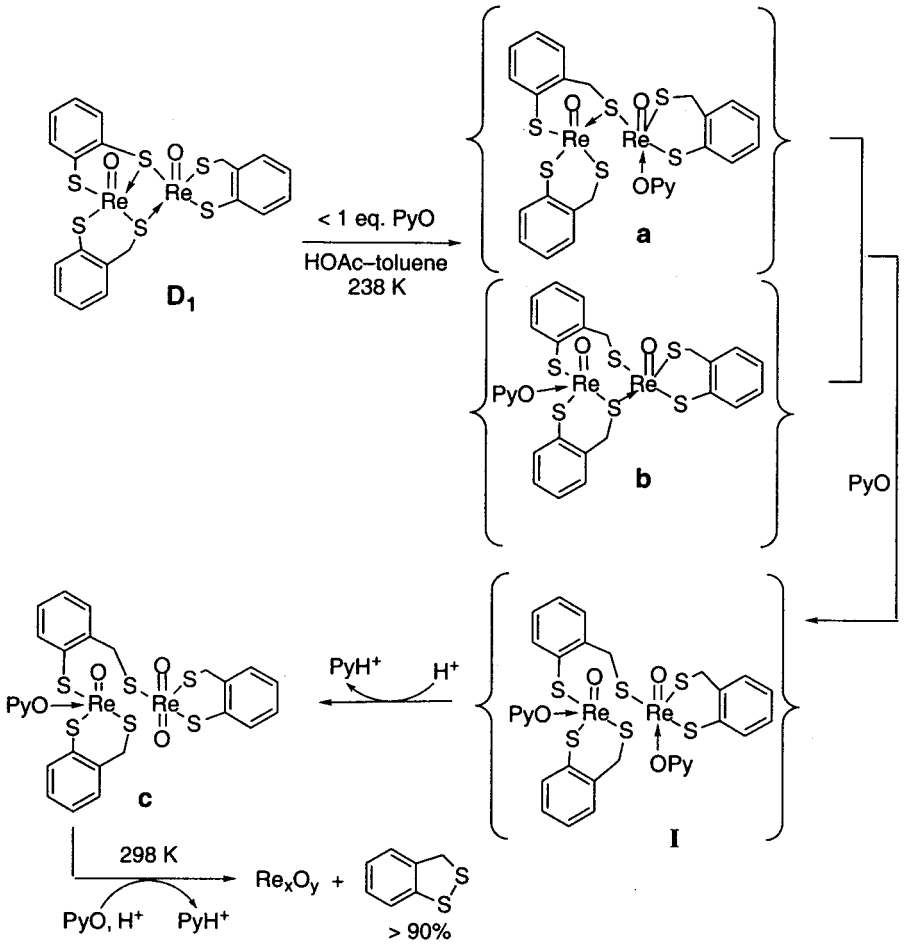

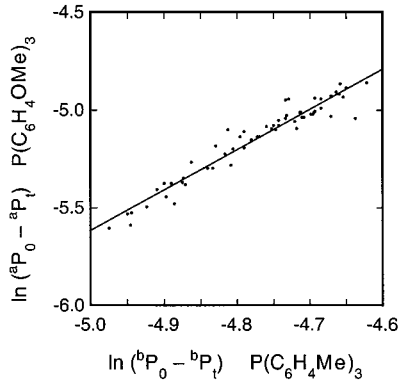

Figure 1. Kinetic data for the concurrent and competitive oxidation reactions of $P(C_6H_4\text{-}p\text{-}OMe)_3$ and $P(C_6H_4\text{-}p\text{-}Me)_3$ by $4\text{-}MeC_5H_4NO$ at 25 °C, as catalyzed by $\mathbf{D_1}$ in benzene under an argon atmosphere at 25 °C. The rate constant ratio is given by the slope of this double-logarithmic plot, according to eq 7. Concentrations used were 0.05−0.10 mM $\mathbf{D_1}$, 30−60 mM PyO, and 2−30 mM of each phosphine.

oxide was determined over time from the integrations of the NMR signals. Each logarithmic term was evaluated and one plotted against the other. An example for the case $P^a = P(C_6H_4\text{-}p\text{-}OMe)_3$ and $P^b = P(C_6H_4\text{-}p\text{-}Me)_3$ is shown in Figure 1. The data define a straight line within the precision of the results, consistent with eq 7. The slope of the line gives the rate constant ratio, in this case with a value of 2.1 in favor of $P(C_6H_4\text{-}p\text{-}OMe)_3$ over $P(C_6H_4\text{-}p\text{-}Me)_3$. To test that this method gives results that are independent of the PyO used, similar experiments were carried out with $4\text{-}NCC_5H_4NO$, using the same pair of triaryl phosphines. As it happens, the rate constant ratio was again 2.1, proving the point.

Table 2. Relative Rate Constants for Oxidation of PAr_3, $AsPh_3$, and $SbPh_3$ by 4-Methylpyridine *N*-Oxide, Catalyzed by $\mathbf{D_1}$, and for Comparison Reactions

			log(k_Y/k_H)		
reagent	$3\sigma_Y$	k_Y/k_H [a]	**PD$_1$**	MeRe-$O(O_2)_2$ [b]	(TMP)-$Ru(O)_2$ [c]
$P(C_6H_5\text{-}4\text{-}OMe)_3$	−0.81	8.57	0.933		0.314
$P(C_6H_5\text{-}4\text{-}Me)_3$	−0.51	5.46	0.737	0.105	0.030
PPh_3	0	(1.000)	0	0	0
$P(C_6H_5\text{-}4\text{-}F)_3$	0.186				0.296
$P(C_6H_5\text{-}4\text{-}Cl)_3$	0.69	1.45	0.161	−0.182	0.372
$P(C_6H_5\text{-}4\text{-}CF_3)_3$	1.62	0.95	−0.022	−0.330	0.248
$AsPh_3$		0.23	−0.638	−0.235	−1.69
$SbPh_3$		0.32	−0.495	−0.140	1.66

[a] Determined according to eq 7. [b] Data from ref 29. [c] Data from ref 30.

Various combinations of P^a and P^b were then used in a pairwise manner, with concentrations and partners chosen so that a balance between the two reactions would be maintained. For $P(C_6H_4\text{-}p\text{-}Y)_3$, the combinations studied were $^aY/^bY$ = MeO/Me, MeO/H, Cl/H, Cl/CF_3, and CF_3/H. The reactivities of $AsPh_3$ and $SbPh_3$ were also determined by the same method except that a 10- to 20-fold excess over PPh_3 was needed, these reagents being considerably less reactive than the phosphine. The rate constant ratios so determined were normalized relative to that for PPh_3 (k_{rel} = 1.000). The values of k_Y/k_H, and of log(k_Y/k_H), are presented in Table 2. Data for two comparison systems are also presented. They are the oxidation of PAr_3 by a peroxo-

Table 3. Kinetic Data (Initial Reaction Rates) for the Oxidation of PAr_3 by 4-MeC_5H_4NO, Catalyzed by $\mathbf{D_1}$, under Argon[a]

$[PAr_3]_0$/ mM	$[PyO]_0$/ mM	$[Py]_0$/ mM	[HOAc]/ mM	$v_i/10^{-7}$ mol L^{-1} s^{-1}
		(a) $P(4\text{-}MeOC_6H_4)_3$		
1.58	64.0			15.4
3.80	64.0			15.0
3.80	35.5			8.3
		(b) PPh_3		
2.56	34.6		100	5.37
6.92	34.5		100	5.74
5.23	41.7		100	6.73
8.00	80.0		100	15.1
6.44	35.0	36.0		1.91
6.44	58.3	36.0		2.94
12.4	58.3	36.0		5.27
12.4	55.8	17.3		10.5
12.0	54.0			11.3

[a] Conditions: under argon at 25 °C in C_6D_6; $[\mathbf{PD_1}] = 1 \times 10^{-4}$ M.

rhenium compound, $MeReO(O_2)_2(OH_2)$,[29] and by the ruthenium porphyrin compound, *trans*-Ru(TMP)$(O)_2$.[30]

O-Atom Transfer: Reaction Kinetics for Triarylphosphines. The kinetics of the reactions of PyO with various phosphines were determined. Some competition experiments were also carried out for $AsPh_3$, $SbPh_3$, Me_2S, MeSTol, 2-methyl-1,3-pentadiene, and cyclohexene. The reactions were carried out in the presence of a catalytic amount of $\mathbf{D_1}$ (<1%); it was confirmed that $\mathbf{PD_1}$ is the only form of rhenium that could be detected during the catalytic oxidations. Control experiments showed that no reaction occurred without the catalyst. Both the disappearance of the substrate and the buildup of the product were monitored by ^{1}H NMR spectroscopy.

For purposes of kinetics two phosphines were used, $P(4\text{-}YC_6H_4)_3$, Y = MeO and H; the pyridine *N*-oxide was 4-MeC_5H_4NO. Data were obtained in benzene at 25 °C under argon. Unlike the competition experiments, phosphines were used separately and not in pairs. Four ^{1}H NMR signals were monitored with time: PAr_3, PyO, Ar_3PO, and Py. The products were formed in a 1:1 ratio, confirming the stoichiometry shown in eq 2. In all experiments, [PyO] was greater than $[PAr_3]$, and both were much greater than $[\mathbf{PD_1}]$, usually set at 1×10^{-4} M. Kinetics data were analyzed by the initial rate method. The initial rate was evaluated at 42−100 μM $[\mathbf{PD_1}]$ with 7.4 mM PPh_3, 90.0 mM PyO, and 100 mM HOAc. The data showed that v_i is directly proportional to the catalyst concentration.

The initial rate data are given in Table 3. For $P(4\text{-}MeOC_6H_5)_3$, the data (Table 3a) clearly show that the initial rate remains independent of the phosphine concentration and directly proportional to the PyO concentration **(**Figure S-3 of Supporting Information). Thus, the rate law is

$$v_i = k_1[\mathbf{PD_1}][\mathrm{PyO}] \tag{8}$$

where $k_1 = 0.24$ L mol^{-1} s^{-1} in benzene at 25 °C. This suggests that the rate is controlled by a reaction between $\mathbf{PD_1}$ and PyO and that PAr_3 enters the reaction cycle at a later and more rapid step. The step with PAr_3 involved directly was studied in the previously described competition experiments using pairs of phosphines. As far as the kinetics go, it is both the concentration of PAr_3 and its rate constant that together determine whether the rate limit given in eq 8 can be sustained.

To test this point, we moved from $P(4\text{-}MeOC_6H_5)_3$, the most reactive of the phosphines, to PPh_3, the least reactive (refer to Table 2). Included in this set (Table 3b) were several experiments in which acetic acid was added to protonate the released pyridine, eliminating any possible effect from it. Another series was then run with 17−36 mM pyridine added, a level higher than would be produced in the reaction. An inhibiting effect of pyridine was evident at the highest concentrations. The initial rates for these experiments take the form

$$v_i = \frac{k_1[\mathbf{PD_1}][\mathrm{PyO}]_0[\mathrm{PPh_3}]_0}{\frac{k_{-1}}{k_2}[\mathrm{Py}]_0 + [\mathrm{PPh_3}]_0} \tag{9}$$

The rate law suggests a scheme of (at least) two reactions. In sketchy form, it is

$$\mathbf{PD_1} + \mathrm{PyO} \underset{k_{-1}}{\overset{k_1}{\rightleftharpoons}} \mathrm{Int} + \mathrm{Py}$$

$$\mathrm{Int} + \mathrm{PAr_3} \xrightarrow{k_2} \mathbf{PD_1} + \mathrm{Ar_3PO} \tag{10}$$

With HOAc present, the first denominator term will be absent; the same is true when the first term is much less than $[PPh_3]$, which is usually so even without added HOAc. Analysis of these data (see Figures S-4 and S-5 in the Supporting Information) affords these values: $k_1 = 0.20 \pm 0.04$ L mol^{-1} s^{-1} and $k_{-1}/k_2 = 0.59$. This value of k_1 differs slightly from 0.24 L mol^{-1} s^{-1} because a different phosphine is present in $\mathbf{PD_1}$; also, the presence of acetic acid may cause a minor medium effect.

O-Atom Transfer: Other Substrates. Sulfides (Me_2S and MeSTol) can be used in place of phosphines in the reaction with 4-MeC_5H_4NO catalyzed by $\mathbf{D_1}$ (<1%). Sulfide oxidation is comparable in rate to the self-oxidation of the mtp ligands of $\mathbf{D_1}$, which stopped the reaction before sulfoxide formation was complete. When $PTol_3$ and MeSTol were used together, with $PTol_3$ just 0.2% MeSTol, no sulfoxide was detected until all the Tol_3PO had been formed. With less than 0.2% $PTol_3$, a mixture of phosphine oxide and sulfoxide was detected. From that we estimate from the ratio of products that $PTol_3$ is ca. 5×10^2 times more reactive than MeSTol (this refers to their relative values of k_2 in eq 10).

An attempt was made to oxidize 2-methyl-1,3-pentadiene with the $\mathbf{D_1}$−PyO combination, but only disulfide from oxidation of the mtp ligand was detected. Another oxidant, di-*tert*-butyl peroxide, was successful with $\mathbf{D_1}$ as a catalyst. With 250 mM peroxide, 25 mM diene, and 2.0 mM $\mathbf{D_1}$, about 30% of the epoxide was formed in 6 h. Cyclohexene was not oxidized under the same conditions.

Discussion

Direct evidence was obtained for these two reactions, as cited previously. Both reactions are very rapid and both occur to completion.

$$\mathbf{D_1} + \mathrm{PAr_3} \rightarrow \mathbf{PD_1} \tag{11}$$

$$\mathbf{PD_1} + \mathrm{Py} \rightarrow \mathbf{PD_1}\mathrm{Py} \tag{12}$$

The structure of $\mathbf{PD_1}$Py was not determined; our suggestion is given in Chart 2 (see also Chart 1). This species can interact with PyO, removing an oxygen atom, thereby oxidizing one of the Re atoms to Re(VII). This generates the important intermediate $\mathbf{PD_1}$(=O)Py, which the data identify as the important

(29) Abu-Omar, M. M.; Espenson, J. H. *J. Am. Chem. Soc.* **1995**, *117*, 272.
(30) Cheng, S. Y. S.; James, B. R. *J. Mol. Catal.* **1997**, *117*, 272−280.

Chart 2. Suggested Structures for the Reaction Intermediates

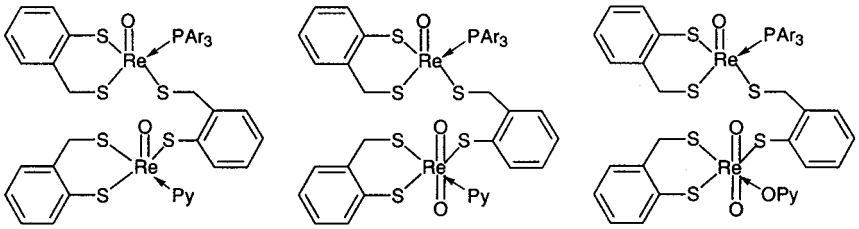

PD$_1$Py **PD$_1$(=O)Py** **PD$_1$(=O)OPy**

recycling form of the catalyst. The chemical equation is

$$\mathbf{PD_1}\text{Py} + \text{PyO} \rightarrow \mathbf{PD_1}(=\text{O})\text{Py} + \text{Py} \qquad (13)$$

This reaction is driven not only by the previously cited preference for PyO over Py as a ligand but particularly by the decrease in Gibbs energy when Re(V) is oxidized to Re(VII) by PyO. The dissociation energies lie in the order Re−O > Py−O. A double-labeling experiment was carried out with YPyO to which XPy was added at the beginning of the reaction. No XPyO was detected at any point, showing that reaction 13 is irreversible. Clearly, once Py has been released, it cannot be reincorporated into any PyO.

The first of two competing rate-controlling steps is also a reaction of PyO important in the kinetics. It is a reversible reaction with Py as a product:

$$\mathbf{PD_1}(=\text{O})\text{Py} + \text{PyO} \underset{k_{-1}}{\overset{k_1}{\rightleftharpoons}} \mathbf{PD_1}(=\text{O})\text{OPy} + \text{Py} \qquad (14)$$

This step represents a PyO-for-Py ligand replacement reaction. It is crucial, giving rise to the species that actually leads to O-atom transfer:

$$\mathbf{PD_1}(=\text{O})\text{OPy} + \text{PAr}_3\ (\text{or X}) \xrightarrow{k_2} \mathbf{PD_1}(=\text{O})\text{Py} + \text{Ar}_3\text{PO}\ (\text{or XO}) \qquad (15)$$

In this step it seems highly probable that the oxygen atom being transferred is not that of Re═O but of Re−O−Py. On the basis of the presumed bond energies, which are not known here but can be roughly estimated from species closely related, B(Re═O) ≫ B(Py−O), the Py−O bond may be weakened further by PyO coordination. Reaction 15 is not limited to the most reactive phosphine reagents but occurs as well for X = $AsPh_3$, $SbPh_3$, Me_2S, and *trans*-3-methyl-1,3-pentadiene. The last two reagents, and perhaps all four, would be unable to abstract an oxygen atom from Re═O. It is not possible, however, to design a labeling experiment because ultimately all oxygen atoms are derived from PyO. These results make it clear that PyO coordination is favored over Py. Aside from phosphines, other substrates that form weaker bonds to oxygen can also be oxidized but not by direct transfer from Re═O. These arguments explain the need for reactions 14 and 15.

A different epoxide is formed from the diene with this rhenium catalyst compared to the result when oxidation occurs with H_2O_2 and with MTO as the catalyst.[31]

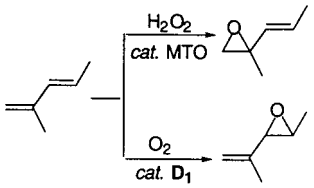

Rate comparisons can be made concerning the group of PAr_3 compounds studied here with two other cases from the literature. One is the H_2O_2/MTO case, where oxidation occurs from a peroxo rhenium group. The other is a reaction in which a Ru═O group of a metalloporphyrin, *trans*-Ru(TMP)$(O)_2$, is attacked directly by PAr_3, $AsPh_3$, or $SbPh_3$. These LFER correlations have been attempted (see Table 2 and Figures S-6 and S-7 in the Supporting Information). Neither correlation, however, is particularly persuasive.

Reaction 15 is accelerated by ring substituents in the series $P(C_6H_5Y)_3$. In terms of electronic influence, the effect is irregular. The rate order (Table 2) follows this rather unusual ordering of Y: MeO > Me ≫ Cl > CF_3 ∼ H. These are the only data, however, and an overinterpretation is hardly justified. In the presumed transition state for reaction 15,

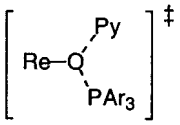

one can easily envisage opposing effects of electron density that could give rise to this trend.

Acknowledgment. This research was supported by the U.S. Department of Energy, Office of Basic Energy Sciences, Division of Chemical Sciences under Contract W-7405-Eng-82.

Supporting Information Available: Plots of kinetic data to illustrate agreement with selected mathematical forms and to evaluate numerical parameters. This material is available free of charge via the Internet at http://pubs.acs.org.

IC000854K

(31) Tan, H.; Espenson, J. H. *Inorg. Chem.* **1998**, *37*, 467−472.